VESPA experiment

Physics laboratory - 29/10/2023
Group 3
Marchesini Davide - 2121242
Lorenzo Frigato - 2109747
Aneesh Suresh Nene - 2004982

1 Abstract

A plasma is by definition a near-neutral ionized gas which shows a collective behavior. It is indeed an extremely complex physical system and at the same time extremely common in our universe, such that more than 99% of the known matter in the universe is made up of it. In this experiment we want to study and characterize not only the main characteristic quantities of a plasma (such as its density, the electronic temperature, the plasma potential and so on) but also the experimental apparatus in which the plasma is created. In order to do so we will start characterizing the vacuum system of our chamber and studying the emission of electron for the Richardson law from the filament inside the chamber. After that we will study the experimental conditions under which a discharge occurs and plasma is created both in AC and DC regime. Subsequently, we will measure the main plasma parameter through the simplest possible diagnostic, a Langmuir probe, and, finally, we will study how the system reacts to an external periodic perturbation that will induce some collective behavior in the plasma, namely ion acoustic waves.

2 Data analysis

2.1 Vacuum production and characterization

In the first place, we want to model the experimental setup. In particular, we are going to create a plasma in a vacuum chamber in low pressure condition. A dynamical equilibrium between the vacuum pump and all the possible leaks and gas sources inside the chamber must be created in order to control the chamber's experimental condition. The latter is described by a balance equation

$$-V\frac{dp}{dt} = Sp - F_0 \tag{1}$$

where F_0 is a cumulative gas flow rate that takes into account all the possible leak sources (degassing, evaporation and so on), S is the pumping speed of the system while p the pressure in the chamber and V its volume. If both S and F_0 are independent from the pressure, one can solve with respect to two different cases. If we leave the pump attached to the chamber

$$p(t) = (p_i - p_0)e^{\frac{-St}{V}} + p_0 \tag{2}$$

where $p_0 = F_0/S$ is the limit pressure and p_i is the initial pressure of the chamber. If instead we isolate the pump from the chamber

$$p(t) = p_0 + \frac{F_0}{V}t \tag{3}$$

Therefore, by taking experimental data of the pressure in function of the time in those two different situations, and making experimental fits, it is possible to characterize completely our experimental set up. Since the time data were taken by timing with the chronometer of the phone, it was taken as an error on time the average time of human reaction, calculated as 0.2 s. Meanwhile, since the pressure wasn't constant, but was oscillating between certain values, as an error of the measured pressure we've taken the first significant digit that stayed the same during the observation time. Since at smaller pressure the oscillation became more evident, we expect that the smaller is the pressure and the bigger is the relative error on it. De facto, in our case, the errors are all the same.
Now a consideration must be made. The latter are just attempts to estimate the data errors. Those are

probably wrong and underestimated, either because the phone's chronometer is not a precise instrument and either because we didn't have the control and the possibility to fully study and characterize our instruments, in particular the ionization gauge. This is a situation that will presents itself again in this experience. Furthermore, assigning arbitrary errors to our data doesn't help even the realization of the experimental fits, since that if the errors in data are all equal they will only change the errors on the fit parameters but not their value. And being that the errors that we assigned, as we already said, are probably wrong, there is no advantage to try to assign an arbitrary error on the data. For this reasons, for now on, when it is possible to estimate a reasonable errors for our data we will try to do it (as in this case), elsewhere we will not, and we will try to report our experimental difficulties in obtaining the data.
Below are presented the graphs of the experimental data and relative fit (Fig 1 and 2), with the results of the fit shown in the table 1:

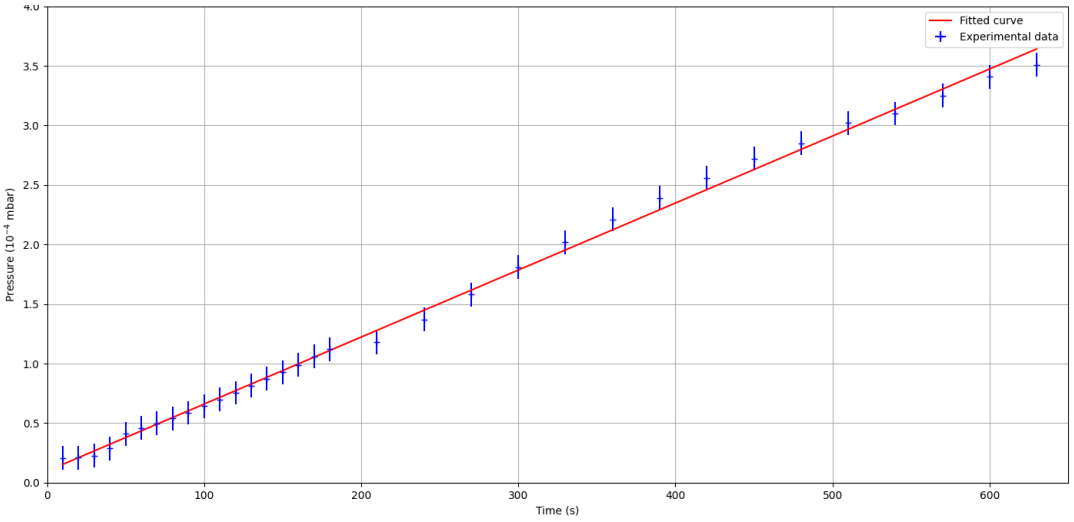

Figure 1: Pressure in function of the time with the valve between the pump and the chamber closed.

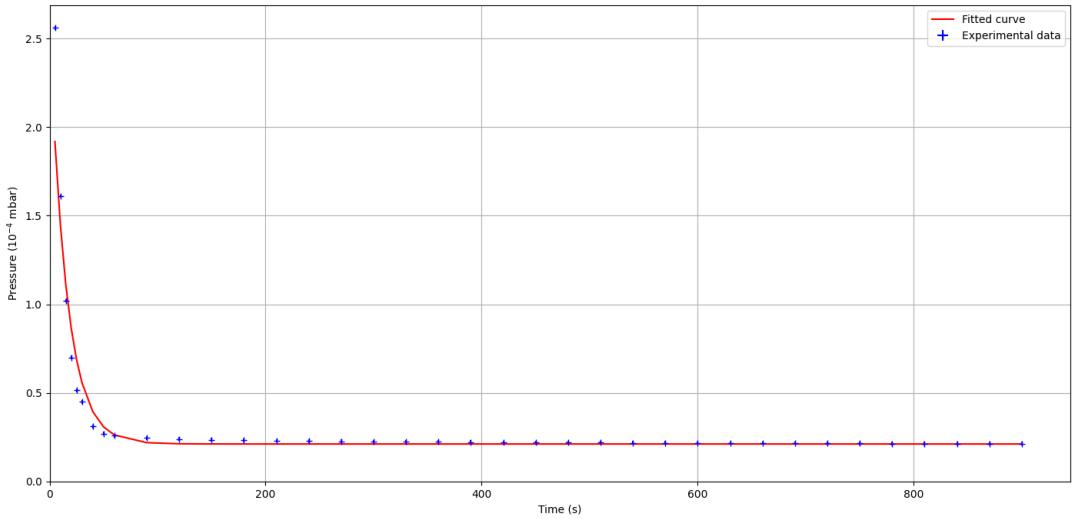

Figure 2: Pressure in function of the time with the valve between the pump and the chamber opened.

Fit parameter	Value	Error
m	$5.63 \times 10^{-7}[mbar/s]$	$0.05 \times 10^{-7}[mbar/s]$
q	$9 \times 10^{-6}[mbar/s]$	$2 \times 10^{-6}[mbar/s]$
p_0	$2 \times 10^{-5}[mbar]$	$0.2 \times 10^{-5}[mbar]$
τ	16 s	1 s

Table 1: Obtained values and errors for the linear and exponential fit parameters.

Here m is the angular coefficient and q is the intercept of the linear fit, while τ is the characteristic time

of the exponential and p_0 was already defined. Since we can take the volume V of the system and a first approximation as the volume of the cylindrical vacuum chamber, that is known, it is possible from the fit parameters to calculate S and F_0. We obtain

Quantity	Value	Error
F_0^{lin}	$2.83 \times 10^{-7}[mbar \cdot m^3/s]$	$0.03 \times 10^{-7}[mbar \cdot m^3/s]$
S	$3.2 \times 10^{-2}[m^3/s]$	$0.2 \times 10^{-2}[m^3/s]$
F_0^{exp}	$6.8 \times 10^{-7}[mbar \cdot m^3/s]$	$0.9 \times 10^{-7}[mbar \cdot m^3/s]$

Table 2: Estimated quantities from the fit parameter.

We notice that the value for F_0 calculated from the linear fit and from the exponential fit are of the same orders of magnitude, even if there is a small discrepancy between their values. This is because we've assumed that S and F_0 were independent of the pressure in order to solve the balance equation. This is not true, and in reality they depend by the pressure of the chamber, that was different in the two cases. One could also compare the effective pumping speed velocity with the nominal one $S_{nom} = 0.033\ m^3/s$: it transpires that the two values are identical within the uncertainties. It is even possible to estimate the conductivity C of the connection between the chamber and the pumping system. If we assume that before opening the valve in the connection there was the perfect vacuum, then $C = (2.65 \cdot 10^{-03} \pm 0.4 \cdot 10^{-03}) \quad m^3/s$.

2.2 Filament characterization

It is also possible to characterize and model the behavior of the tungsten wire. As a first approximation it is possible to consider it as a cylindrical non-ideal black body (with radius r and leght L) at the ends of which a potential difference is applied. Being V_f and I_f the filament applied potential and currents, the characteristic of the filament is given by

$$V_f(I_f) = \left(\frac{CL}{\pi r^2}\right)^{\frac{10}{7}} \left(\frac{1}{\alpha\epsilon 2\pi r L}\right)^{\frac{3}{7}} I_f^{\frac{13}{7}} = \lambda I_f^{\frac{13}{7}} \Rightarrow I_f(V_f) = \left(\frac{V_f}{\lambda}\right)^{\frac{7}{13}} \tag{4}$$

where ϵ is the tungsten effective emissivity, α is the Stefan-Boltzman costant and $C = 6.2 \times 10^{-11} K^{\frac{5}{6}} A^{-1} m^{-1}$ it is an empirical constant. It is possible to see that the experimental data match relatively well with this simple model (is found $\epsilon \approx 0.24$), as shown in fig. 3.

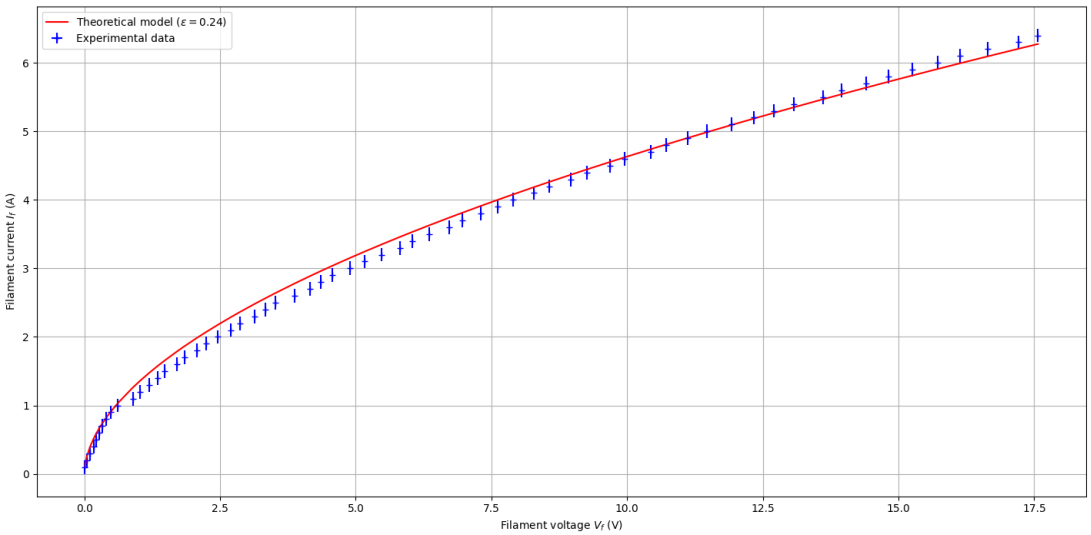

Figure 3: Experimental data taken to construct the filament characteristic and the theoretical prevision by our simple model.

The experimental data were taken by collecting different values of the voltages of the filament by changing its current. Here we try to estimate the errors on the I_f and V_f by using the last significant digit of the measuring instrument, even if there is no need in terms of data analysis. Thanks to the simple filament

theoretical model, it is also possible to estimate the filament temperature T in function of its driven current

$$T(I_f) = \left(\frac{\lambda}{\epsilon\alpha 2\pi r L}\right)^{\frac{1}{4}} I_f^{\frac{5}{7}} = \Gamma I_f^{\frac{5}{7}} \tag{5}$$

Therefore it is possible to estimate the filament temperature for our experimental $(V_f; I_f)$ data, which will growth as a power law, as shown in fig 4.

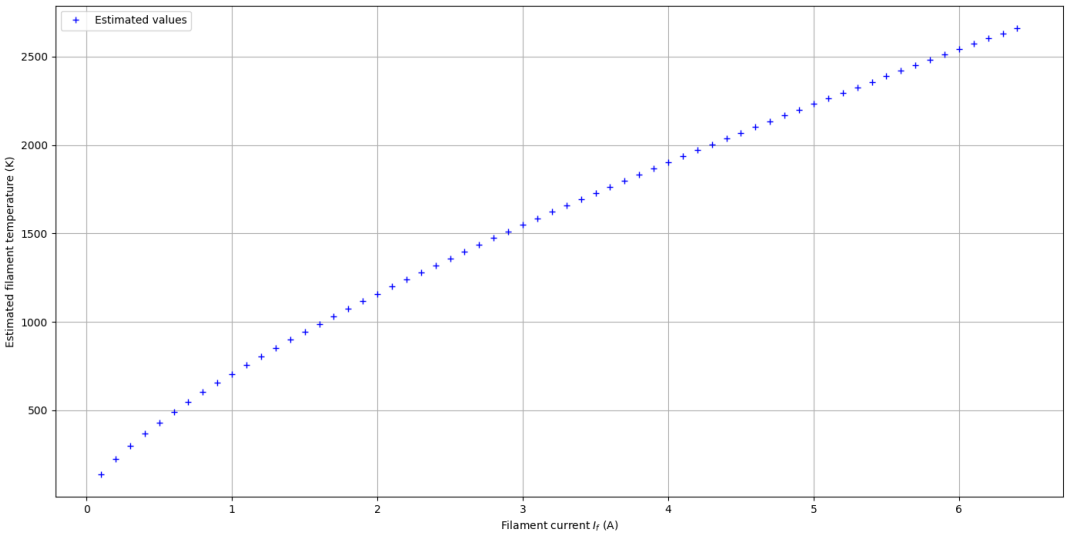

Figure 4: Estimated filament temperature as a function of its driving current.

2.3 Breakdown discharge: Voltage-Current characteristic

To characterize the discharge we have to firstly study its voltage-current characteristics, from which we can estimate the breakdown voltage V_b of the filament. We define it as the voltage for which one (experimentally) sees a sudden rise on the current values, meaning that the discharge has happened and the plasma is ignited. The characteristic curve is experimentally found, first by varying current supplied to the filament and later, by changing the pressure of the gas in the vacuum tube. The pressure maintained for the first part of the analysis was $p \approx 2 \times 10^{-3} mbar$, and by varying the applied voltage between the chamber and the filament, the current values for the plasma were noted through a 1Ω shunt resistor. This was done for multiple current values, keeping the same pressure. For the second part of the analysis a constant current of $I_F = 6.5A$ was supplied to the filament and the procedure was repeated by varying the pressure. The observed voltage-current characteristics after varying the current and the pressure, separately, are given below in figure 5 and figure 6 respectively. The values for the breakdown voltage obtained are given in the table below. In the

Filament Current	Breakdown Voltage
6.0 A	30.0 ±0.1 V
6.3 A	31.9 ±0.1 V
6.5 A	32.2 ±0.1 V
6.6 A	31.8 ±0.1 V

(a) Breakdown voltage for different values of current

Pressure ($10^{-3} mbar$)	Breakdown Voltage
2.0	32.2 ±0.1 V
4.0	30.4 ±0.1 V
8.0	29.0 ±0.1 V

(b) Breakdown voltage for different values of pressure

first case, on increasing the filament current, no significant change in the breakdown voltage was observed (as we expected, because to ignite the plasma we need electrons with enough energy in order to ionize the atoms. Then, provided that we have a minimum number of electrons to begin the chain reaction, i.e. a certain minimum value of the current filament, changing the filament current, only change their number over the minimum requested. But now what is really important is no more their number, but their energy, i.e. V_b), whereas in the second case, on increasing the pressure in the chamber, the breakdown voltage was reduced. This could be related to the fact that increasing the gas density it is easier to have ionization because there will be more collision (it is important to remember than only a fraction of the collision gives ionization. Other possible outcomes could be excitation of the atom, recombination etc.). In particular we

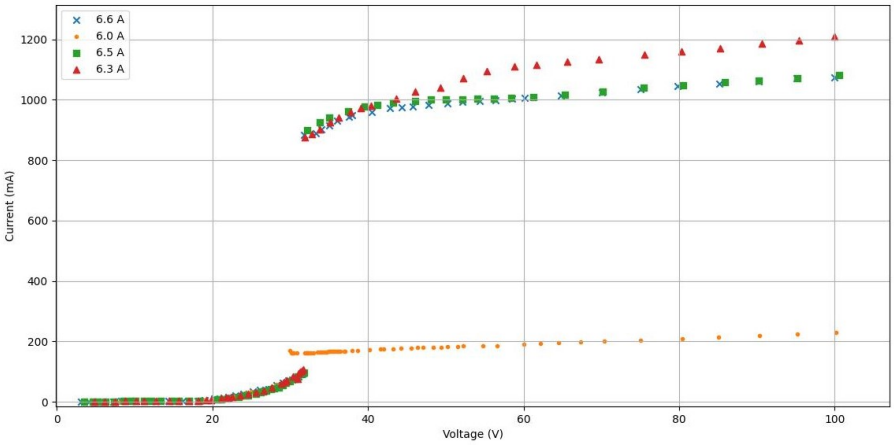

Figure 5: Voltage current characteristic for various filament current values at constant pressure

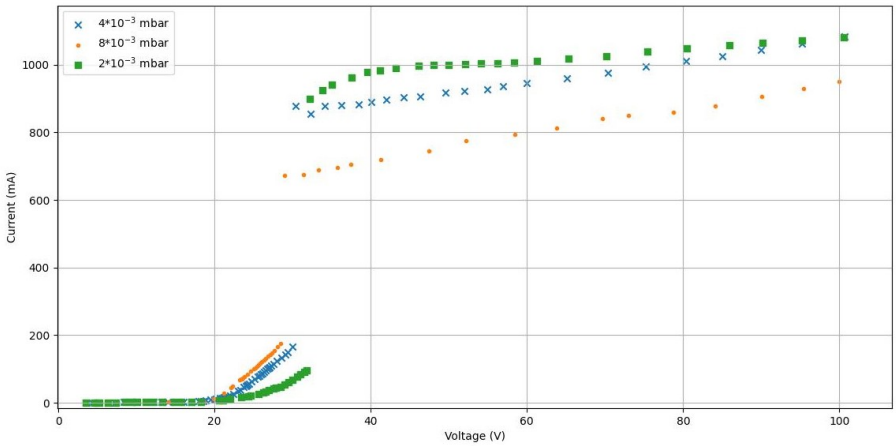

Figure 6: Voltage current characteristic for various pressure values and constant filament current

are on the left branch of the Paschen curve, as can be seen in fig 7. It is important to note while studying the voltage-current characteristics, one peculiar thing was observed. The current applied to the filament reduced in value, after the breakdown voltage was reached. The reason behind this could be, since at breakdown voltage, plasma is formed and part of the current flowing through the filament flows through the polarization circuit, where we observe a sudden rise in current. The plasma plays a role of the carrier of that part of the current, from the filament circuit to the polarization circuit.
In table 3, we have compared the discharge current obtained at 60 V polarization voltage, for various values of filament current, with the ones obtained by Richardson's law, i.e.

$$I_e = A\Gamma^2 I_f^{\frac{10}{7}} \pi r^2 L \cdot exp\left(\frac{-e\phi}{k\Gamma I_f^{5/7}}\right) \tag{6}$$

where ϕ is the tungsten's extraction potential and A a constant. It is evident that the observed values of

Filament current (A)	Observed discharge current (A)	Predicted current by Richardson's law ($10^{-5}A$)
6.0	0.19	2.14
6.3	1.11	4.67
6.5	1.01	7.61
6.6	1.00	9.62

Table 3: Observed vs predicted discharge current by Richardson's law

discharge current at 60 V is much higher than predicted values of emitted current by the Richardson's law. The reason behind this is, at 60 V (much above the breakdown voltage) the plasma has been created and

the electrons emitted by the filament by thermionic emission are accelerated and hit the atoms of Argon gas and ionise them and excite electrons in the Argon atoms. These electrons are accelerated again across the potential difference applied and we get a chain reaction of electron emissions, thus giving a larger observed current than the emitted current by the filament as predicted by the Richardson's law. There is indeed a multiplication of the current by a factor $10^4 - 10^5$.

2.4 Breakdown discharge: Paschen curve in DC

Paschen's law provides an empirical relationship between the breakdown voltage (V), the pressure (p) of the gas, the distance between the electrodes (d). After experimentally acquiring the breakdown voltage, the Paschen curve is plotted and as expected, it has a minimum, as can be seen in 7. The minimum of the curve chosen is the minimum value observed before a slight increase and then the flattened curve is observed. The observed minimum by the Paschen's curve is for $p_{min} \approx 4.8 \times 10^{-4} mbar$.

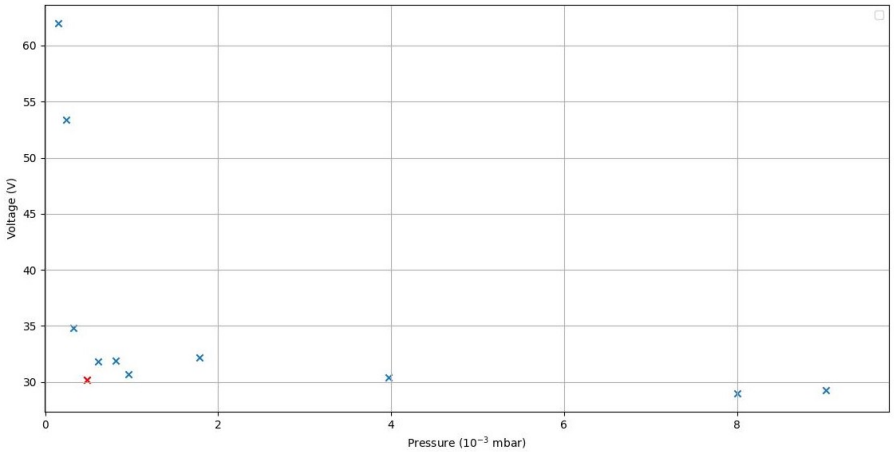

Figure 7: Paschen's curve for plasma in DC

It is important to note, in our investigation, we have examined the deviations between our empirical Paschen curves and the theoretical model. The Paschen curve offers valuable insights into the behavior of breakdown potential, which is contingent upon the product of pressure and distance. In our specific experimental setup, the distance represents the separation between the cathode and anode of the filament and the chamber. When we maintain a constant value for the product $p \cdot d$ we observe consistent behavior within the system, resulting in nearly identical values for the breakdown voltage. However, it is also important to note that in the context of our experiments, we lack precise control over the value of d, which represents the inter-electrode distance. Conversely, we do possess control over the pressure p within the chamber. Consequently, the system autonomously adjusts the combination of $p \cdot d$ to produce the observed breakdown voltage 'V_{bd}'. When pressure remains relatively stable, the distance also exhibits minimal variation, thereby yielding only slight fluctuations in V_{bd}. Conversely, under conditions of higher pressure, the electron current seeks a more direct path to complete the circuit. This results in a shorter d, while the product of $p \cdot d$ remains largely constant. Consequently, V_{bd} does not increase as one might intuitively expect. The variability observed, particularly in the vicinity of the curve's minimum, is attributable to the system's adaptive nature. It is capable of positioning itself within the minimum by adjusting the interplay of pressure and distance, sometimes leading to values of V_{bd} that appear anomalously higher or lower, as evident in our data.

2.5 Paschen curve in radio frequency condition

A similar study of voltage dependence on pressure was studied using the Paschen's curve in radio-frequency conditions. To apply high enough voltages to the chamber so as to achieve a plasma without the use of the filament, the resonant response of an RLC circuit was exploited to sinusoidal signals, produced through a waveform generator. To begin, we characterised the resonant frequency of the of the circuit using an oscilloscope. The plot of voltage vs frequency is shown in figure 8. The maximum was observed at $f \approx 3.96$ MHz.

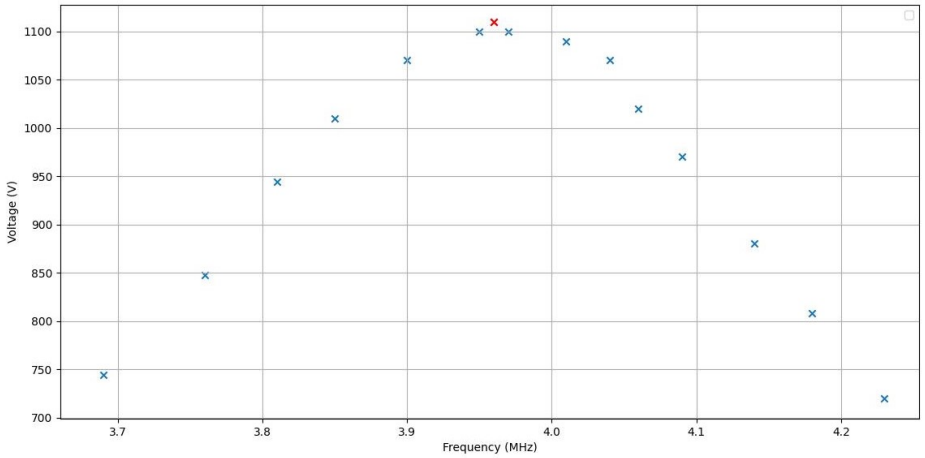

Figure 8: Resonance curve for the RLC circuit

At this frequency, values of pressure and breakdown voltage were experimentally found by varying the oscillation frequency. Using these values, the Paschen's curve was plotted as shown in figure 9. The minimum of the curve chosen is the minimum value observed before a slight increase and then the decrease of the curve is observed. The minimum of this Paschen's curve is observed at $p_{min} \approx 1.95 \times 10^{-2} \quad mbar$

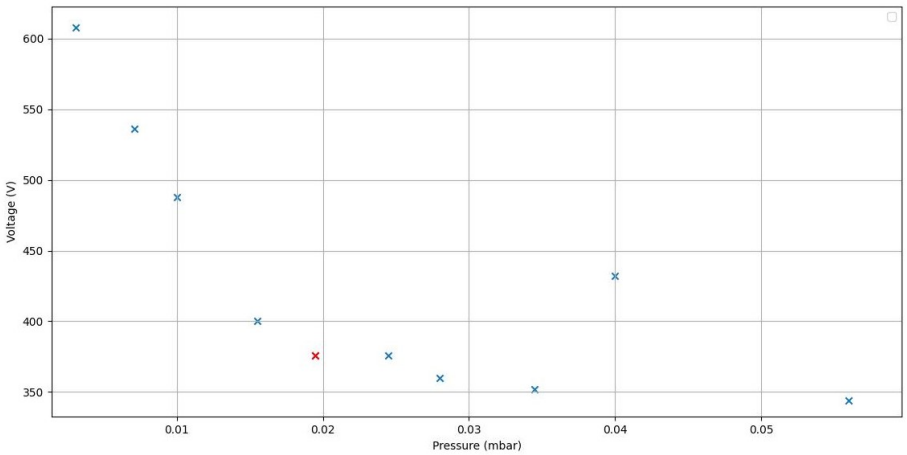

Figure 9: Paschen's curve for plasma in RF

Comparing voltages observed in DC mode with the ones observed in RF mode, it can be concluded that the voltages in DC mode are much lower than the ones in the RF mode. This is due to the presence of the filament in the DC mode, which, with thermionic emission of electrons, helps the plasma to start the ionisation process, whereas in case of RF mode, ionisation is induced only by applying high voltages which allows the free electrons already present in the plasma (due to cosmic rays for instance) to oscillate. It is also possible to see the same "flat" behaviour exhibited at the minimum, that was already discussed in the DC part.

2.6 Plasma characterization

With the term characterization of the plasma it is intended the measurement of some fundamental parameters that describe the state of the plasma. The Langmuir probe is the easiest instrument that performs this operation. In our case two probes are present, one called NEAR, that is indeed near the filament inside the chamber, and the other one called FAR, positioned on the opposite side. The position is indeed important because the plasma does not present uniform characteristics in the entire chamber. To measure the plasma's parameters the Langmuir probe modifies its own voltage and measures the net current that flows throw itself. By doing so it is possible to create a characteristic graph of the curve $I(V)$ and to perform a four

parameter fit with the function

$$I(x) = I_{is} \cdot [1 + R \cdot (x - V_f)] \cdot (\exp \frac{x - V_f}{T_e} - 1) \tag{7}$$

where the parameters have a corresponding physical value as: I_s is the ionization saturation, R a shape parameter of the curve, V_f the floating potential, at which the function is zero and T_e the temperature of the electrons. From this fit parameters it is also possible to obtain the plasma density n and the plasma potential V_{plasm}. Since the Langmuir probe is a plasma diagnostic that perturbs the system by measuring it, in order to obtain reliable measurements, it is necessary to make some preliminary steps before the data analysis. The latter were automatically performed by the Python fit program provided to us in the laboratory. Different data run acquisitions have been performed with both the probes, where we were able to estimate the value of the five plasma parameters (in every plot the blue dots represent the NEAR probe while the orange dots the FAR one). It is important to report that the data acquisition for four different conditions were not as good as the others (the four data at higher and lower pressures and the radio frequency data). Using the Python program installed in the laboratory computer, the fit was not even executed because the plots were extremely deformed. In figure 10 we provide an example of a normal graph on the left and one deformed on the right. Luckily the following fit parameters do not present high error parameter so we can confirm that the fit is correctly executed and that the curves are simply more different that the expected ones.

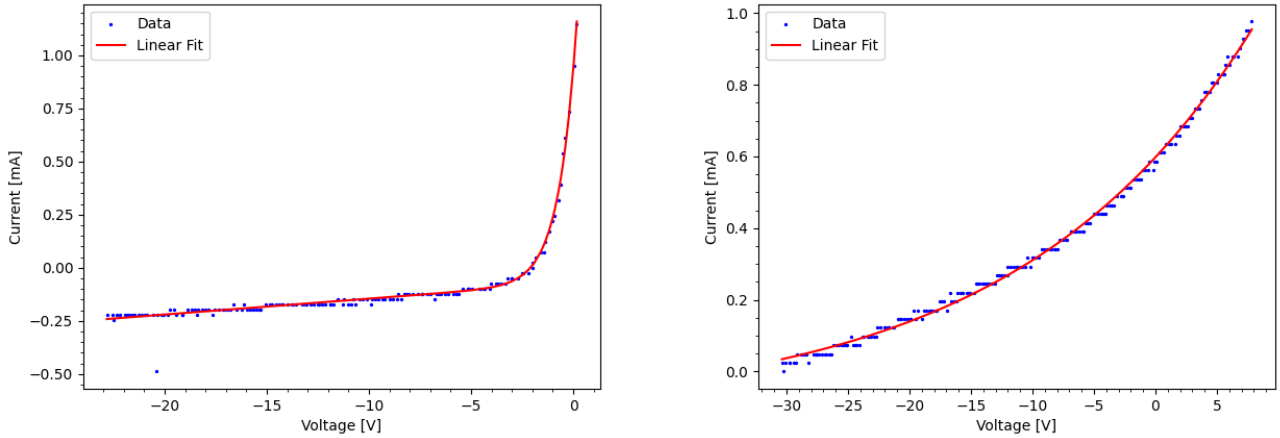

Figure 10: A fit for the normal and deformed curve

So, one data run has been acquired with the pressure fixed at around $p = 5 \times 10^{-4} mbar$ and by changing the discharge voltage we obtained the plasma parameters that are plotted in figure 11. It is possible to notice some trends:

1. The plasma current increases as the discharge voltage applied increases, as described in the previous sections (we collected also this data for completeness)

2. The floating potential and the plasma potential seems to remain constant as the discharge voltage is increased (there is no significant trend). But it is also possible to see that $V_f - V_{plasm} < 0$ always. This could mean that the plasma, or better its external region, the so called Debye sheet, is positively charged, since in the beginning it loses electrons that will hit the probe due to their higher mobility. This mean that the probe is instead negatively charged, until a point in which the Colombian repulsion between the electrons prevents other electron to come and a flux of ion is instead obtained, until eventually an equilibrium is reached, so the net current is zero. The potential of the probe it is now indeed the floating potential V_f.

3. We would expect also to observe a positive correlation between the voltage and the plasma density, since we expect that if V grows it would be easier to ionize the gas. This is indeed the case for the FAR probe, while for the NEAR we see a sudden drop in the plasma density between 40 and 50 volts. Also the ion saturation current seems to follow this trend, and this is reasonable since the two quantities are correlated.

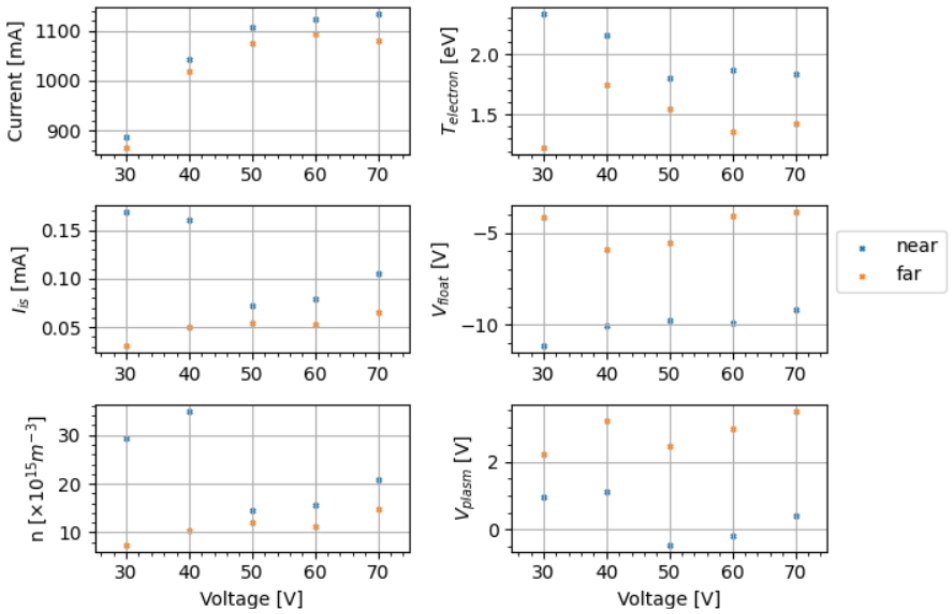

Figure 11: Plasma parameter in functions of the discharge voltage (pressure fixed).

4. We would expect to observe a positive correlation between the voltage and the temperature of the electrons (i.e. their kinetic energy) but this trend is not clear and instead it seems rather the opposite. Since the pressure is constant this can't be attributed to the change in the mean free path but maybe could be attributed to the fact, that since the plasma density increases, and therefore the collisions between the different species increases, it is more difficulty to gain energy.

5. It is clear that a discontinuity in trend in the density and I_s behaviour is present passing from the values at $40V$ and $50V$ (also for the V_{plasm} parameters) which indicates that a possible problem had occurred, not in the fits because they have been controlled, so directly on the data (it is not possible to say more). The solution for this problem could be the error on the parameters but we know that they are of the order of $1 - 10\%$ the value, so it isn't.

6. As it has been said before, the NEAR and FAR probes measure different parameter values because the plasma is more enhanced near the filament. It is possible to see that there is a clear difference between the two data sets and, in addition, one of the two data sets is always above (or below) the other, for the same discharge voltage.

One run was acquired maintaining the discharge voltage fixed at around $V = 70V$ and changing the pressure by an order of 10 obtaining the results in the plots in figure 12. It is possible to notice some reasonable trends:

1. In this case the trends of the parameters are easier to visually appreciate compared to the previous plots. This is because changing the pressure it means to change the density of the gas and consequently of the plasma itself, that leads more appreciable differences.

2. The electron temperature decreases as the pressure increases because the mean free path of the electron decreases, and so the electron are not allowed to be accelerated as in a less dense gas medium.

3. The plasma density increases as the pressure increases because there are more collisions in the gas at higher pressure and the plasma is enhanced easily. This explain also why the floating potential increases and the plasma potential instead decreases with the increase of the pressure: if the plasma (and the neutral gas) density is higher, less electrons can reach the probe due to collisions, leaving a less positively charged plasma.

4. it is possible to notice that for some values the difference between the NEAR and FAR probe is nearly null and the dots are interposed, this indicates that the specific plasma parameter in this case is more uniform in the chamber

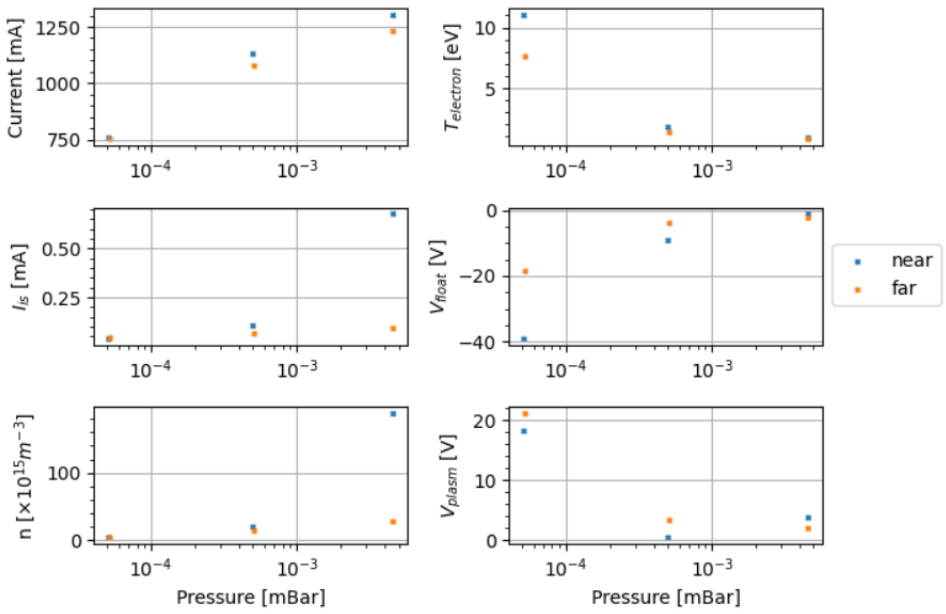

Figure 12: Plasma parameter in function of the pressure (V constant). It is important to note the logarithmic scale in the x-axis.

And the last run acquire was performed using the radio frequency generator at a pressure of $P = 2.15 \cdot 10^{-2} mBar$, which is the experimental minimum of the Paschen curve in RF, and at a voltage peak to peak observed in the oscilloscope of $V = 960mV$.

Position probe	$T_e[eV]$	$I_{is}[mA]$	$V_f[V]$	n $[\times 10^{15} m^{-3}]$	$V_{plasm}[V]$
FAR	4.83	0.037	3.68	4.85	28.69
NEAR	10.67	0.054	-0.33	4.80	54.98

Table 4: Data collected by using the RF generator.

For all the data set it is possible to calculate the ionization fraction as $f = n/(n + n_0)$ where n is the plasma density calculated by the Langmuir probe and, using the perfect gas law, $n_0 = P/(k_B T)$ where the temperature considered, is the ambient temperature of $293.15K$. We obtain the results:

Position probe	Voltage [V]	ionization fraction [%]
FAR	30	0.061
FAR	40	0.085
FAR	50	0.097
FAR	60	0.092
FAR	70	0.120
NEAR	30.1	0.253
NEAR	40.0	0.296
NEAR	50.0	0.124
NEAR	60.0	0.129
NEAR	70.1	0.171
	Pressure $[\times 10^{-5} mbar]$	
FAR	5.2	0.391
FAR	50.4	0.120
FAR	451.0	0.025
NEAR	5.1	0.278
NEAR	49.5	0.171
NEAR	458.0	0.167
	Radio frequency	
FAR		0.000912
NEAR		0.000903

Table 5: Ionization fraction for all data sets.

2.7 Ion acoustic wave propagation

In this part we will analyze the generation of the so-called Ion Acoustic sound waves. This operation has been performed by applying an oscillating potential on the grid located in the middle of the vacuum chamber at $f = 20KHz$. The potential accelerates the electrons and thanks to the long range electromagnetic interaction a periodic oscillation is produced. We settled the pressure at a value around $p = 5 \times 10^{-4} mBar$ and discharge voltage of $V = 70V$. Then data on the amplitude of the wave and phase difference, between the produced signal in the grid and the measured by the system, thanks to a mobile Langmuir probe positively polarized at $+50V$ and connected to a resistance of $10K\Omega$. At the end of this resistance we measured the wave signal amplitude and phase. So we collected data modifying the distance, thanks to a manipulator, obtaining the results in the table:

Relative distance [cm]	Amplitude [mV]	Phase difference [$\times 10^{-6} s$]
1	100	-6.523
2	165	-3.066
3	160	1.200
4	177.2	5.200
5	173.2	9.334
6	175.7	13.47
7	161.7	17.33
8	148	20.76
9	136	23.6
10	102.4	27.2
11	70.6	30.53

Table 6: Data collected by changing the distance and measuring the amplitude and phase difference.

The phase difference between the two signals is described by the linear formula $x = a \cdot \phi + b$ in which the slope is the propagation velocity c_s^*.

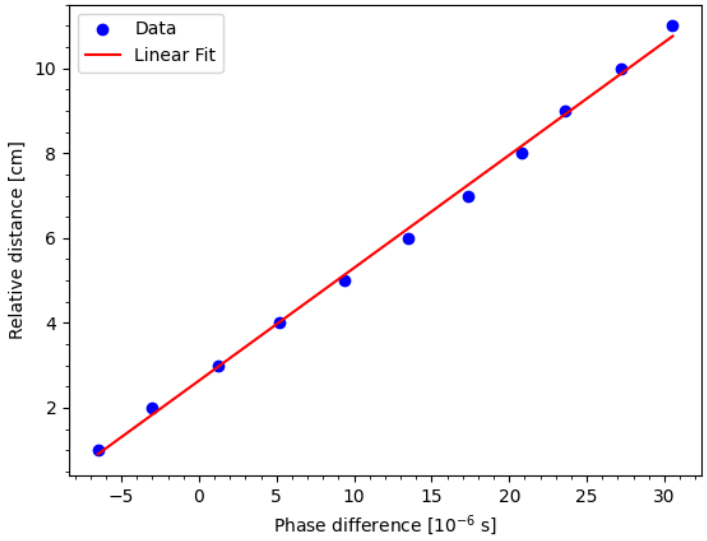

Figure 13: Linear fit.

We performed the fit obtaining the following results. (Here errors are not taken into account. This is because in the laboratory it wasn't so clear how to take them, since there was a very large oscillation of the curve visualized in the oscilloscope. Furthermore we are more interested in the fit parameters values rather than their errors).

$$a = (0.266 \pm 0.004) \frac{cm}{10^{-6} s} = (2.66 \pm 0.04) \times 10^3 \frac{m}{s} \quad b = (2.64 \pm 0.08) cm \tag{8}$$

It is also possible to calculate the ionic sound wave velocity using the data obtained in the previous section and the equation $c_s^* = \sqrt{(k_B \cdot T_e)/m_{Ar}}$, with $m_{Ar} = 39.9 \times m_p$ (with m_p the proton mass). In the end, the results for the same pressure and discharge voltage conditions are:

$$c_s^{NEAR} = 2.104 \times 10^3 \frac{m}{s} \quad and \quad c_s^{FAR} = 1.850 \times 10^3 \frac{m}{s}$$

The oscillation has a amplitude that, as a function of the distance, is described by an exponential decay, i.e. $A = A_0 \cdot e^{-\delta \cdot x}$, with δ the dampening length parameter, that is related to the neutral particle density as

$$\delta = \frac{c_s^*}{v_{te} n_0 \sigma_0} \Rightarrow n_0 = \frac{2a}{\delta v_{te} \sigma_0}$$

where the velocity calculated via the previous fit can be used. The fit has been performed only for the last 6 values and an error of $10mV$ has been considered for the amplitudes, because during our data collection the oscilloscope value was badly oscillating causing the impossibility to set a specific value. Observing that the value was always in the interval of confidence of $10mV$, we chose this value as a guess for the errors.

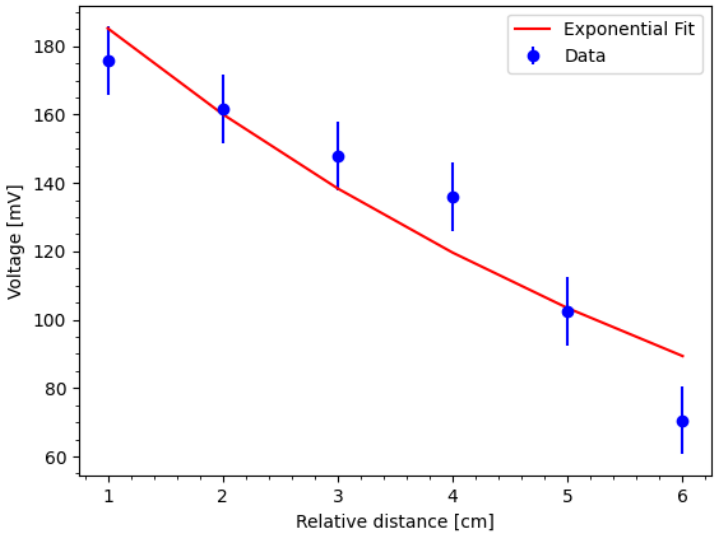

Figure 14: Exponential fit.

We obtain the results

$$A_0 = (214 \pm 18)mV \quad \delta = (0.15 \pm 0.03)cm^{-1} \tag{9}$$

Assuming that the Argon gas has an electron temperature of around $1eV$ (which has been verified in the previous section, at the specific pressure of of $5 \cdot 10^{-4} mbar$) the neutral cross section is around $2 \times 10^{-20} m^2$ and with $v_{te} = \sqrt{(8k_B T_e)/(\pi m)}$, the value of the neutral density is $n_0^{exp} = 2.35 \cdot 10^{20} \quad m^{-3}$. This value is greater than the expected one using the perfect law gas, which is around $n_0^{law} = 1.3 \cdot 10^{19} \quad m^{-3}$, but considering the errors in the measurement of the damping length it is an obvious consequence.

3 Conclusion

In conclusion, we successfully studied and characterized our experimental set up: both our models for the vacuum chamber and the tungsten filament have proven to be accurate, even in their simplicity. We've identified the best pressure conditions -i.e. the minimum of the Paschen curve - to have the discharge in our chamber (in DC and AC conditions) even though, as discussed, the impossibility of having experimental access to the distance between the electrodes allows us to verify only a partial section of the behaviour of the entire theoretical Paschen curve. We have also been able to characterize the plasma under different experimental conditions, verifying trends and correlations between the different physical quantities involved. This was also the most difficult part of the analysis, due to the great experimental difficulties encountered in acquiring sensible data with Langmuir probes. The sources of these errors were not clear and probably need further investigation. Finally, the plasma perturbations have been studied successfully, even though the great experimental instabilities and fluctuations on the data acquired.